Available online at www.sciencedirect.com

ScienceDirect

Physics Procedia 60 (2014) 356 – 362

Physics Procedia

Union of Compact Accelerator-Driven Neutron Sources (UCANS) III & IV

Quantitative evaluation of imaging characteristics of the neutron image intensifiers

H. Ishikawa[a*], T. Kamiyama[a], K. Nittoh[b], M. Yahagi[c], and Y.Kiyanagi[a]

[a]*Guraduate School of Engineering, Hokkaido University, Japan*
[b]*Toshiba Nuclear Engineering Service Corporation, Japan*
[c]*Toshiba Power Systems Inspection Services Co., Ltd, Japan*

Abstract

A vacuum-tube type neutron image intensifier (NII), composed of Gd or ^{10}B neutron convertor, is considered to have better spatial resolution and better detection efficiency compared with a traditional neutron scintilator. However, quantitative evaluation of difference in sensitivity among these imagers and difference in characteristics of the images between two NIIs has not been done since it needs measurements under the same irradiation condition. In this study we carried out radiography experiments at Hokkaido University Neutron Source (HUNS). Firstly, neutron radiography images were obtained by Gd-type NII, ^{10}B-type NII, and the traditional neutron scintillator; NE426 (ZnS:Ag/^{6}LiF). Next, we evaluated the brightness values from these images. We also evaluated the contrast and the image quality from two NIIs. The brightness of Gd-type NII is 8.8 times and the ^{10}B-type is 12.9 times higher than the NE426. There is contrast little difference between the two types of NII. The image quality of Gd-type is better than ^{10}B-type when exposure time is short.

Peer-review under responsibility of the Organizing Committee of UCANS III and UCANS IV

Keywords: neutron image intensifier; transmission imaging; neutron radiography; HUNS.

1. Introduction

Neutron imaging is a method of non-destructive inspection and has unique characteristics such as high penetrating power and high sensitivity to hydrogen and light elements compared with X-ray. For the traditional imaging, various neutron converters have been developed and used. Recently, we have been developing counting type imagers [1-3] that can be used at pulsed neutron sources, namely that have a function of the time-of-flight measurement. Another imaging device candidate is vacuum-tube type neutron imaging intensifiers (NII) [4] since it has been considered to have high detection efficiency and high spatial resolution compared with the traditional neutron scintillator NE426 (ZnS:Ag/^{6}LiF). These

* Corresponding author. Tel.: +81-11-706-7896; fax: +81-11-706-7896.
E-mail address: hirotaku-ishikawa@eng.hokudai.ac.jp.

Peer-review under responsibility of the Organizing Committee of UCANS III and UCANS IV
doi:10.1016/j.phpro.2014.11.048

characteristics are preferable for using at pulsed neutron sources. Therefore, we are developing a camera type imager using the NII developed by Toshiba Co. [5]. There are two types of NII, the first is Gd-type, which has gadolinium as a converter material, and the second is ^{10}B-type, which has boron-10 as a converter material. The detail of NIIs is described in the chapter 2.1.

The recognized characteristics of NIIs is the higher efficiency than usual devices [4], however, quantitative evaluation of efficiency of NIIs and the traditional scintilator has not been performed. Hence, although there are two types of NII, we have only known the imaging property roughly. Therefore, to use each NII property depending on the experimental condition we should know the characteristics of the image obtained with them.

For the primary subject of this study is quantitative evaluation of two NIIs and traditional scintillator NE426 (ZnS:Ag/^{6}LiF), and their characterization in images as basic information for the NII usage at pulsed neutron sources.

2. Experimental

2.1. NII structure

Fig. 1 shows the structure of NII and details of its input window of two types. Firstly the NII converts incident neutrons into electrons at the input window as shown in the Fig. 1. Converted electrons are accelerated and converged by the electron lens. In the output screen the converged electrons are converted to photon with $Y_2O_2S_2$:Eu [5], and make the photo image. Finally, the photo image is captured by a digital camera for recording.

The input window with Gd-type converter consists of an Al base plate, 12 μm thickness Gd_2O_3 film, 50 μm thickness CsI film and photoelectric conversion film. In the Gd_2O_3 film, the (n, γ) reaction and internal conversion occur. For γ-ray, since it has high energy, very few γ-ray reaction occurs in the CsI film. Then the electron conversion occur mostly and deposit its energy $h\nu$ in the CsI film, where h is the Planck's constant and ν is the frequency. The CsI film has the many fine pole structure which crosses to the surface, and the structure guides the produced photon to the photoelectron film with small divergence. That makes the NII maintain the high spatial resolution. The thickness of CsI film is determined based on the range of conversion electron. The input window with ^{10}B-type converter consists of an Al base plate, 5 μm $^{10}B_4C$ film, 20 μm thickness CsI film and photoelectric conversion film. The (n, α) reaction occurs in the $^{10}B_4C$ film, then α-particle deposits the energy to the CsI film and makes photons. The thickness of CsI film is determined based on the range of α-particle.

All the reactions in the input windows have own quantum efficiency, and the efficiency of the converter varies with neutron energy. Hence, the total efficiency of the two NIIs is different. The evaluation of their efficiency is difficult due to the complexity of the NIIs.

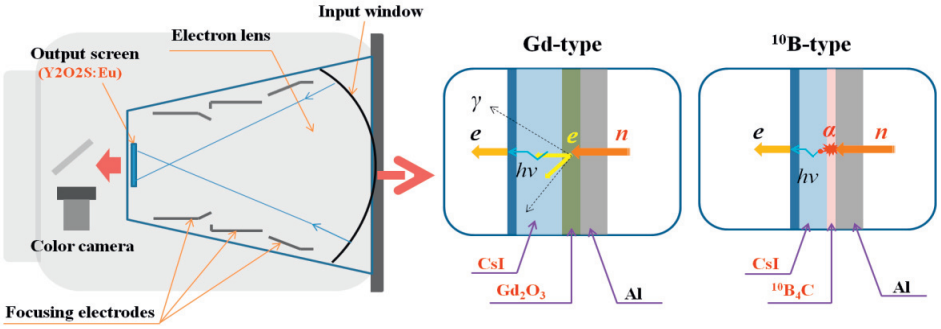

Fig. 1. NII apparatus structure and schematics of the two NII converters.

2.2. Experimental setup

Radiography experiments were carried out at Hokkaido University Neutron Source (HUNS), which was a compact electron accelerator-driven neutron source. Fig. 2 shows a schematic layout of the experimental setup. The setup consisted of the neutron source, a collimator, a sample and imaging system. The distance between the moderator surface on the source and the detection surface of the imaging system was 4.5 m. The arrangement of the source, the collimator and the sample was fixed. The present source was a cold neutron source using a coupled methane moderator. The cold neutron flux was 1.52×10^4 n/cm^2/s at the detection surface.

The imaging system was changed for the each measurement. The first of imaging system was the combination of each NII and a digital camera. In contrast, the second of one was changed the combination of the usual neutron scintillator, NE426 (ZnS:Ag/^{6}LiF) and the same camera. The combined digital camera was the comercialed Canon EOS 5D mark II, and its ISO sensitivity was set as 800. The camera exposure time was changed as 10 s, 30 s, 60 s, 120 s and 300 s in every measurement of using the another NII imaging systems. When using the NE426 imaging system, only 1800 s were used for the camera exposure time.

The measured sample was a character plate and the ASTM indicator. The latter was standard indicator used for neutron radiography [6, 7].

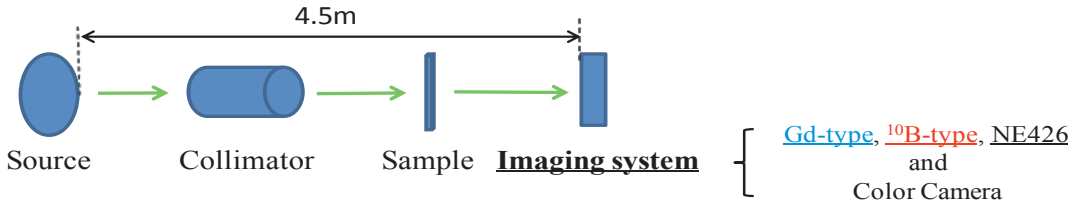

Fig. 2. Schematic layout of the experimental setup.

2.3. Evaluation method

The images were evaluated on three criteria: brightness (efficiency), contrast, and image quality. Fig. 3 shows the sample measured and a corresponding image produced by the ^{10}B-type NII. The ASTM indicator included a beam purity indicator (BPI), which we used in the image evaluation. Brightness values were obtained using image processing software by Toshiba co. Averaged brightness from the two regions of interest (denoted by rectangles in Fig. 3 (b)) were used for determining the contrast. The two averages were termed “Hole brightness of BPI” and “BN disc brightness of BPI” as in the Fig. 3 (b). For determining the contrast, the ratio was calculated as

$$\textit{Contrast ratio} = (\textit{Hole brightness of BPI}) / (\textit{BN disc brightness of BPI}) \quad (1)$$

Moreover, we evaluated the image quality simply by comparing the radiograms by own eyes.

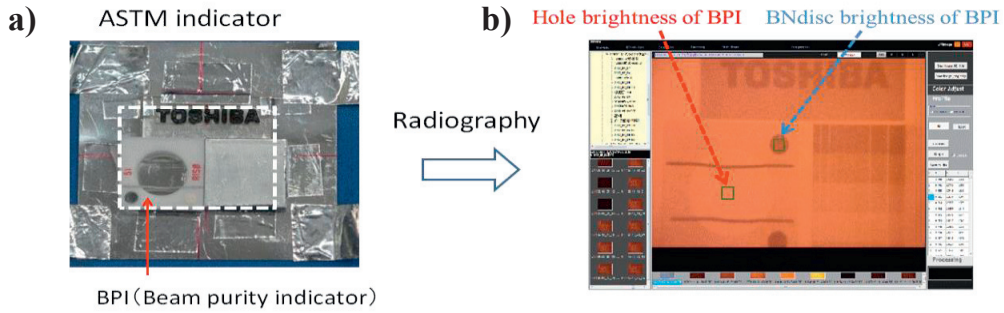

Fig. 3 a) Measured ASTM sample and b) corresponding image produced by ^{10}B-type NII with the 300 s camera exposure time.

3. Results and discussion

3.1. Radiography results

The exposure times were determined by a trial-and-error process during the experiment. Fig. 4 compares the radiography images produced by this process. For the NIIs, the images gradually brighten with increasing exposure time. Below 120 s exposure time, the image brightness is not satisfactory. For t = 120 s and t = 300 s the brightness becomes appropriate and the images are easily recognizable. At t = 1800 s the NII images are totally saturated and not recognizable. The NE426 image can measure at t = 1800 s.

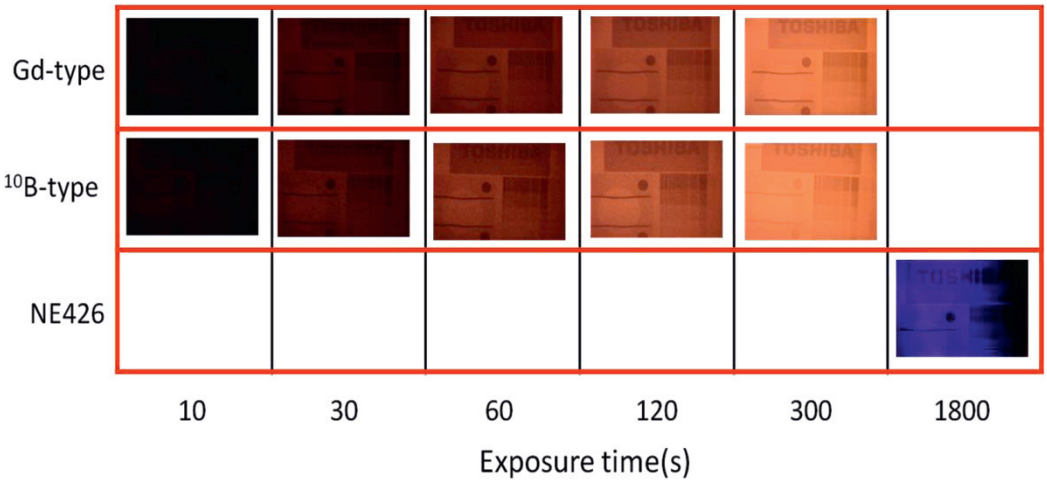

Fig. 4. Radiograms obtained by both NIIs and the scintillator NE426 at different exposure times.

3.2. Efficiency evaluation

Fig. 5 shows the comparison of the change in brightness, which is evaluated from the hole brightness of BPI of the two NIIs with exposure time variation, and also includes the brightness of the traditional scintillator at = 1800 s. The ^{10}B-type is brighter than the Gd-type for all measurements up to 300 s exposure times. The shape of the brightness curves for both NIIs suggests that the rate of increase in

brightness becomes slower with the longer exposure time. This is considered due to the camera sensor property termed the gamma factor. The input-output property of the commercial digital camera sensor does not have a linear property because of adapting the feeling manner of human eyes, and determined by the gamma factor. The input-output property is showing as below,

$$(OUTP) = (INP)^{\gamma} \tag{2}$$

where *OUTP*, *INP*, and γ is the values of the camera output intensity, the light input intensity and the gamma factor, respectively. We define the relative efficiency to compare the time for obtaining the same brightness with the NE426. From Fig. 5, the Gd-type NII can obtain the same brightness of NE426 at 205 s, and the ^{10}B-type 140 s. Comparing these times with NE426 exposure time (1800 s), the Gd-type is 8.78 and ^{10}B-type is 12.9 times more efficient than NE426, respectively. Similarly, comparing these two NIIs, the ^{10}B-type is 1.46 times more efficient than the Gd-type. This efficiency comparison was made under the similar condition for three systems, but it was not the correctly same condition. Therefore, it should be noted the difference in these efficiency is the approximate values. Anyway, it can be said that the efficiency of the NII is nearly one order higher than that of the NE426.

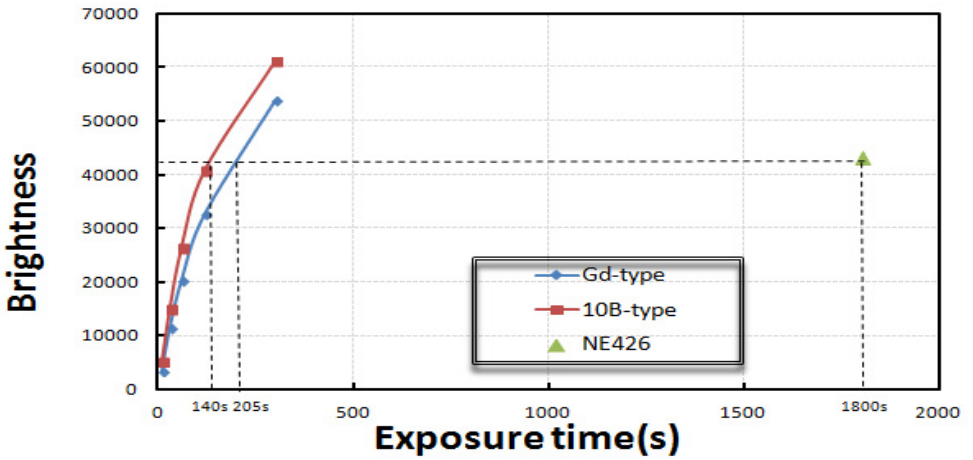

Fig. 5. Exposure time dependence of brightness for both NIIs and scintillator NE426.

3.3. Contrast evaluation

Fig. 6 shows the change of contrast ratios depending the camera exposure time for both NIIs. Below 120 s exposure time, the image quality is very poor (later described in section 3.4), however the contrast ratio of the ^{10}B-type is greater than the Gd-type for these times. Their contrast ratios are crossing around t = 120 s and that of the ^{10}B-type becomes smaller. This is due to the saturating property of the brightness of the ^{10}B-type compared to the Gd-type. The cause of decreasing contrast ratio with increasing exposure time is also due to the the gamma factor as mentioned before.

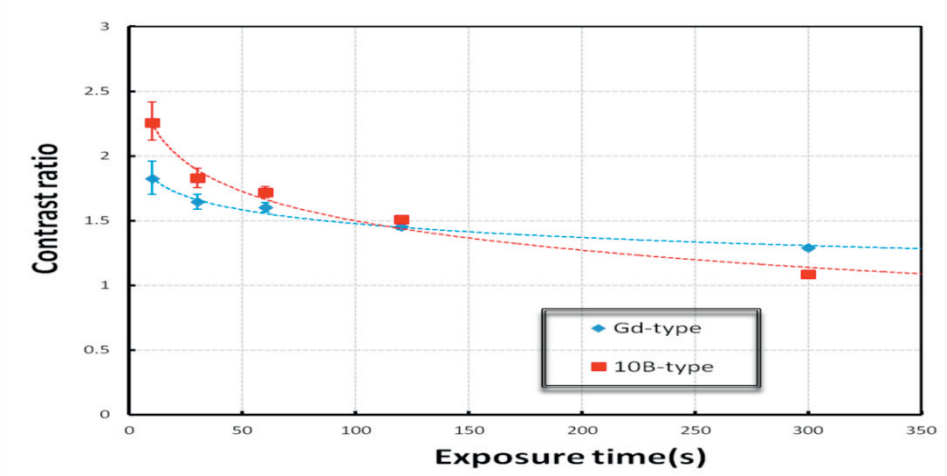

Fig. 6. Comparison of contrast ratios with increasing exposure time for both NII.

3.4. Image quality studies

Fig. 7 shows the two enlarged radiograms focusing in characters on the sample, using both types of NII with 120 s exposure time. The image processing was performed on these radiograms so that one can compare the image quality with ease by own eyes. Images which were obtained below 120 s exposure time were not enough for the image quality recognition distinctly, then we performed image processing. The Gd-type is clearly better in image quality at 120 s. It was found that Gd-type is better in image quality at short exposure times, however at 300 s there is little difference between Gd-type and ^{10}B-type. This is caused by the difference of neutron converters. In the ^{10}B-type, because the range of α-particles is shorter than that of conversion electrons, the energy deposition area by α- particles becomes smaller than that by electrons. Hence, since CsI screen is intensively luminous in small areas by one α-particle, radiograms become more spotted than the Gd-type. Additionally, The neutron absorption ratio is different between two NIIs and are measured about 40% in Gd-type and 15% in ^{10}B-type assuming the cold neutron source of HUNS. Thus, the quantum efficiency of ^{10}B-type is rather small, and there are smaller luminous spot than Gd-type. Therefore, image quality becomes worse in short exposure time. If number of α-particles increase, that is to say, exposure time increase, difference in image quality will become little.

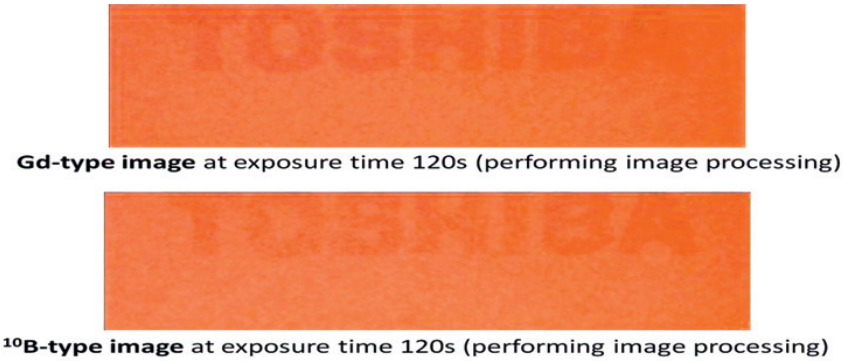

Fig. 7. Comparison of image quality for both NIIs obtained with 120 s exposure time.

4. Conclusion

Radiography experiments were performed in order to make quantitative and qualitative evaluations between Gd-type and ^{10}B-type under three criteria: efficiency (brightness), contrast, image quality. Quantitative comparisons were also made between NIIs and traditional neutron scintillator, NE426.

The brightness of the ^{10}B-type was higher than the Gd-type for all measurements up to 300 s exposure time. The efficiency was evaluated by comparing the times to get to the same brightness of the NE426 and the Gd-type was found to be approximately 8.8 times higher than NE426, and the brightness of ^{10}B-type is 12.9 times. Comparing the two times of two NIIs, the ^{10}B-type is 1.46 times brighter than the Gd-type.

The contrast ratios of the Gd-type and the ^{10}B-type are identical at 120 s exposure times, and contrast does not appear to be an important factor as the change of contrast with exposure time is similar for both NIIs. For the image quality the Gd-type NII produced better than that of the ^{10}B-type NII in short exposure time. These conclusions, are useful for correct choose of the NII depending on a measurement requirement.

Acknowledgements

This work was partially supported by a Grant-in-Aid for Scientific Research (S) from Japan Society for the Promotion of Science (No. 23226018).

References

[1] N. Sakamoto, Y. Kiyanagi, S. Sato, H. Sagehashi, M. Furusaka, J. Suzuki, K. C. Littrell, C. K . Loong, A. Gorin, I. Manuilov, A. Ryazantsev, K. Kuroda, K. Sakai, F. Tokanai, T. Adachi, T. Oku, K. Ikeda, H. Miyasaka, S. Suzuki, K. Morimoto and H. M. Shimizu, J. Appl. Crystallogr., **36**, 820 (2003).

[2] K. Mizukami, S. Sato, H. Sagehashi, S. Ohnuma, M. Ooi, H. Iwasa, F. Hiraga, T. Kamiyama and Y. Kiyanagi, Nucl. Instr. Meth., **A529**, 310 (2004).

[3] S. Uno, T. Uchida, M. Sekimoto, T. Murakami, K. Miyama, M. Shoji, E. Nakano, T. Koike, K. Morita, H. Satoh, T.Kamiyama, Y. Kiyanagi, Phys. Proc., **26**, 142 (2012).

[4] K. Nittoh, Toshiba Review, **64**, 70 (2009).

[5] K. Nittoh, C.Konagai, T. Noji and K. Miyabe, Nucl. Instr. Meth., **A605**, 107 (2009).

[6] ASTM Designation, E545-91 “Standard Method for Determining Image Quality in Direct Neutron Radiographic Examination” (1991).

[7] Riso National Laboratory, RISO-M-2356 “Standardization Activities of the Euratom Neutron Radiography Working Group” (1982).